

# Effects of Ice on Slant path earth-space radio communication links

**Antonio Martellucci<sup>(1)</sup>, J.P.V. Poiaraes Baptista<sup>(2)</sup> and Giulio Blarzino<sup>(3)</sup>**

<sup>(1)</sup>ESA ESTEC, PO Box 299, NL-2200 AG Noordwijk, The Netherlands  
Tel: +31-71-565-5603, Fax: +31-71-565-4999, e-mail: [Antonio.Martellucci@esa.int](mailto:Antonio.Martellucci@esa.int)

<sup>(2)</sup>ESA ESTEC, PO Box 299, NL-2200 AG Noordwijk, The Netherlands  
Tel: +31-71-565-4319, Fax: +31-71-565-4999, e-mail: [Pedro.Baptista@esa.int](mailto:Pedro.Baptista@esa.int)

<sup>(3)</sup>Politecnico di Milano, Dip. Elettronica ed Informazione, Piazza Leonardo da Vinci 32, 20133, Milano, Italy

## INTRODUCTION

The design of multimedia satellite communication systems requires full exploitation of channel bandwidth, To this end the polarisation diversity can be used. A severe limitation is represented by the atmospheric depolarisation, with particular regard to ice crystals in clouds and rainfalls, as also confirmed by the OLYMPUS and ITALSAT propagation experiments. The cloud ice total content has been identified as the most relevant climatic parameter for ice depolarisation. This parameter can be derived from vertical profiles of meteorological data, like that measured by radiosonde or produced by numerical models for weather forecast. The former are characterised by a better spatial coverage, time sampling and consistency of data quality.

## MODELLING OF DEPOLARISATION DUE TO ICE

The atmospheric depolarization can be described in a general way using the transmission matrix,  $\mathbf{T}$ , (a 2x2 complex matrix) that relates the received electric field to the transmitted one [1]. The eigenvectors of  $\mathbf{T}$  (characteristic polarisation) are geometrically orthogonal elliptical polarizations that can be described using the complex canting angle,  $\Phi$ . The real part of  $\Phi$  represents the inclination of the polarizations with respect to the reference system. When the imaginary part of  $\Phi$ , related to the axial ratio of the ellipse of polarization, is equal to zero the characteristic polarizations are linear.

The eigenvalues of the matrix  $\mathbf{T}$  represents the propagation constants of the characteristic polarizations and the anisotropy of the medium,  $\Delta$ , is defined as the difference between the propagation constants.

The following equation gives the complex crosspolar discrimination ratio,  $\delta$ , of linear and circular polarizations

$$\delta_{xy,jx} = -\tanh(\Delta/2)\text{sen}(2\Phi)/[1 \pm \tanh(\Delta/2)\cos(2\Phi)] \quad ; \quad \delta_{rl,lr} = -\tanh(\Delta/2)\exp(\pm j2\Phi) \quad (1)$$

where:

$XPD_{ij} = 20 \log|1/\delta_{ij}|$  = Crosspolar discrimination when transmitting polarization  $j$  and receiving polarization  $i$   
 $r$  = right handed circular polarization ;  $l$  = left handed circular polarization ;  $x$  and  $y$  = linear polarization

The anisotropy can be theoretically calculated using the microphysical properties of atmospheric particles. Although the ice particles are characterised by a large variability of shape and size, they can be classified as needles or plates [2]. The anisotropy due to ice clouds can be estimated using a simple model that assumes cloud composed of ice needles lying on the horizontal plane [3,4]. It can be assumed that the ice needles are maintained aligned onto the horizontal plane by aerodynamic and electrostatic effects, and can rotate freely on this plane. The apparent canting angle is real is given by:

$$\Phi(\gamma) = \arctan[-\cot(\gamma) \cdot \sin(\beta)] \quad (2)$$

where:  $\gamma$  = Horiz. Rotat. angle of the symmetry axis of the needle w.r.t. propagation direction;  $\beta$  = elevation angle

Using this simple model the ice anisotropy,  $\Delta_i$ , depends on the total ice content,  $I$  [mm]

$$\Delta_i(I) = \Delta_{\max}(I) \sqrt{B^2 + C^2} \quad (3)$$

where :  $\Delta_{\max} = j \frac{(\epsilon - 1)\pi}{\lambda} I (c_2 - c_1)$  = Maximum of ice anisotropy when all the needles are aligned

$B = \sin(\beta) \langle \sin[2(90 - \gamma)] \rangle$  ;  $C = \langle \cos[2(90 - \gamma)] \rangle - 0.5 \cos^2(\beta) \langle \cos[2(90 - \gamma)] - 1 \rangle$  ; for details see [1].

$\langle \rangle$  = Ensemble average of the parameter.

$$c_1 = \frac{1}{1 - (\varepsilon - 1)a_1} \quad ; \quad c_2 = \frac{1}{1 - (\varepsilon - 1)a_2} \quad ; \quad a_1 = \frac{m}{2(m^2 - 1)} \left[ m - \frac{1}{2\sqrt{m^2 - 1}} \ln \left( \frac{m + \sqrt{m^2 - 1}}{m - \sqrt{m^2 - 1}} \right) \right] \quad ; \quad a_2 = 1 - 2a_1$$

$\varepsilon = \varepsilon_r - j\varepsilon_i = n^2 =$  Complex permittivity

$m = a/b > 1$  ;  $a, b =$  major and minor semi-axis of the particle

The size distribution of ice particles in clouds can be described using a Gamma function whose modal diameter is characterised by a large spread of values. For cirrus clouds it can be assumed to be lower than 100  $\mu\text{m}$  [5].

The uncertainty related to the ice particle dimensions can be reduced using the cloud temperature, according to the results of drop spectra measurements in mid-latitude and tropical climates, performed using imaging probes mounted on cloud penetrating aircrafts [6,7].

Ice particles on the top of rainfalls, in particular in convective precipitation, are characterised by more complex shapes and orientations with respect to ice crystals in clouds, but the Rayleigh approximation can still be used in the 20/30 and the 40/50 GHz frequency bands. Experimental assessment of ice depolarisation, performed using the OLYMPUS and the ITALSAT satellites [8], evidenced a statistical correlation between the rain attenuation and the ice anisotropy. Additional data and model analysis are required to extend this result to other climatological regions.

According to this model of depolarisation due to ice particles in clouds and rain cells, the atmospheric total ice content represents the required input to the propagation models.

### CLIMATOLOGICAL DATABASES FOR ICE DEPOLARISATION

The European Centre for Medium-Range Weather Forecasts (ECMWF) has carried out operational global numerical weather forecasts since 1979. The data used in this analysis is the one resulting from the assimilation of all available data and then used to initialise the forecast model. It represents the best estimate of the state of the atmosphere. The data covers a period of two years with a time resolution of 6 hours and a spatial resolution 1.5 deg in both latitude and longitude, resulting in 121x240 grid points. The data contain surface pressure and 23 pressure levels of temperature and specific humidity. The typical maximum height of data is about 16 Km.

In order to derive the ice density from the ECMWF database, it has been used the Salonen model for cloud estimation [9]. The original model parameters have been modified to take into account the temperatures lower than -20 C and recent results of propagation measurements. The cloud is detected using the critical humidity:

$$U_c(P) = 1 - \alpha\sigma(1 - \sigma)[1 + \beta(\sigma - 0.5)] \quad (4)$$

where :  $\sigma = p/p_0$  ;  $p, p_0 =$  atmospheric pressure at the considered level and ground pressure ;  $\alpha = 1.0$ ;  $\beta = \sqrt{3}$

Within cloud layers the water density  $w$  [ $\text{g}/\text{m}^3$ ], is a function of the height,  $h$  [m] and of the air temperature,  $t$  [C]:

$$w(t, h) = w_0 \cdot \left( \frac{h - h_b}{h_r} \right)^\alpha \cdot \begin{cases} (1 + ct) & ; t \geq 0 [C] \\ \exp(ct) & ; t < 0 [C] \end{cases} \quad (5)$$

Where  $w_0 = 0.17$  [ $\text{g}/\text{m}^3$ ];  $c = 0.04$  [1/C] ;  $h_r = 1500$  [m] ;  $h_b =$  cloud base height [m]

The liquid and solid water density,  $w_l$  and  $w_i$  [ $\text{g}/\text{m}^3$ ] are given by:

$$w_l(t, h) = w(t, h) \cdot p_w(t) \quad ; \quad w_i(t, h) = w(t, h) \cdot [1 - p_w(t)] \quad (6)$$

Where:  $p_w(t) = \begin{cases} 1 & 0 < t \\ 1 + t/20 & -20 < t < 0^\circ\text{C} \\ 0 & t < -20 \end{cases} =$  Fraction of cloud liquid/ solid water.

The data processing accuracy has been tested comparing the ITU-R database of reduced cloud liquid content [10] with current results. As well the effect on the estimation of the profile resolution has been checked. The validity of the ECMWF data vertical range and resolution of the for the ice cloud estimation has been verified determining the ice cloud top height. Moreover radiosonde profiles [11] have been used for site-specific comparisons.

Values of ice total content exceeded for percentages of annual time ranging from 70 to 0.1 % for each grid point have been calculated. Fig. 1 shows the global map of ice total content exceeded for 0.5 % of the year.

As discussed in the previous chapter, the size of ice crystal in clouds can be related to the cloud temperature. Therefore the statistics of ice cloud top temperature have been determined. For the 50 % of ice clouds, the cloud top temperature is

lower than -10 C and ranges between -30 and -40 C, in the tropical belt and at high-latitudes respectively. As well global statistics of ice cloud height, cloud width and liquid/ice fraction have been derived.

The statistics of ice total content derived from the ECMWF data have been compared with the ice total content estimated using the 50 GHz propagation beacon of the ITALSAT satellite [8]. In fig. 2, the comparison between the statistics of the cloud ice total content, estimated using the ITALSAT measurements of ice anisotropy performed in Pomezia, Italy, and the statistics derived from ECMWF data, is shown. The ITALSAT based estimation of the ice total content has been performed using two extreme hypotheses of the alignment of ice particles. ECMWF based estimation of ice total content has been derived from original grid points using bilinear interpolation. Although the cloud detection model does not discriminate between spherical and non-spherical particles, while measurements are affected only by non-spherical particles, the agreement appears adequate for depolarisation assessment.

## ESTIMATION OF XPD DUE TO ICE CLOUDS

Using the proposed physical model and climatological data, the ice Cross-Polar Discrimination (XPD) can be determined for continental areas. An example is shown in fig. 3, for the 1 % of the year over Europe. It is assumed that communication satellite is located at 13 deg E and that it employs a circular polarization at the frequency of 50 GHz. At this percentage of time rain depolarisation can be discarded but ice depolarisation appears to be relevant, in particular over Northern Europe.

## CONCLUSIONS

Further model development is related to the analysis of available propagation measurements, with particular regard to the interaction between rainfall and ice particles. The new climatic maps derived from ECMWF profiles can be used for ice depolarisation assessment and agrees with independent measurement performed using the ITALSAT propagation beacon. The accuracy and the parameters of the Salonon model for the cloud liquid and ice estimation, can be further improved and investigated, with particular regard to the tropical belt, using local propagation and remote sensing measurements.

## ACKNOWLEDGMENTS

The authors wish to thank Dr. Marina Boumis, Fondazione Ugo Bordoni, Roma, Italy for helpful discussion and suggestions on the analysis of meteorological data.

## REFERENCES

- [1] A. Martellucci (editor), *COST 255 Final Rep., Chapter 2.4, Rain and Ice Depolarisation*, ESA Publication Division, The Netherlands, ISSN: 0379-6566, ISBN : 92-9092-608-2.
- [2] Pruppacher, Klett 1980, *Microphysics of clouds and precipitation*, D. Roidel Publishing Company
- [3] Amaya C., "Depolarisation due to the troposphere and its impact on satellite-to-earth communications", *PhD Thesis, Université Catholique de Louvain, Belgium, June 1995*
- [4] Paraboni A., A. Martellucci and R. Polonio, "A probabilistic model of rain and ice depolarisation based on the experimental estimation of the atmospheric ice content", *Proceed. Of 1997 SBMO/IEEE Intern. Microw. and Optoelect. Conf.*, Natal, Brazil, 11-14 August 1997, pp 707-712
- [5] Ulaby F., Moore R. K., Fung A.K., 1986, *Microwave Remote sensing: From theory to applications*, Artec House Inc.
- [6] Illingworth A. J., C-L Liu, Astin I., Richards B. "Study of the critical requirements for a cloud radar" *Final Report ESA/ESTEC Contract 11326/95/NL/CN*, 1995
- [7] Brown P.R.A., Illingworth A. J. Heymsfield A.J., McFarquhar G.M., Browning K. A. and Gosset M., 1995, "The role of spaceborne millimeter wave radar in global monitoring of ice cloud", *J. Appl. Meteorology*, 34, 2346-2366.
- [8] Martellucci A., Paraboni A. and Filipponi M. "Measurements and modeling of rain and ice depolarization on spatial links in the Ka and V frequency bands" *AP2000 Millennium Conf. on Antennas and Propag.*, Davos, Switzerland, 9-14 April 2000.
- [9] Salonon E. et al., "Study of propagation phenomena for low availabilities", *Final Report ESA/ESTEC Contract 8025/88/NL/PR*, 1990
- [10] ITU-R, Rec P. 840-3, Attenuation due to clouds and fog, 1999
- [11] J.P.V. Poyares Baptista (editor), *COST 255 Final Rep., Chapter 3.2, Precipitation, Clouds and other related Non-Refraction Param.* ESA Publication Division, The Netherlands, ISSN: 0379-6566, ISBN : 92-9092-608-2.

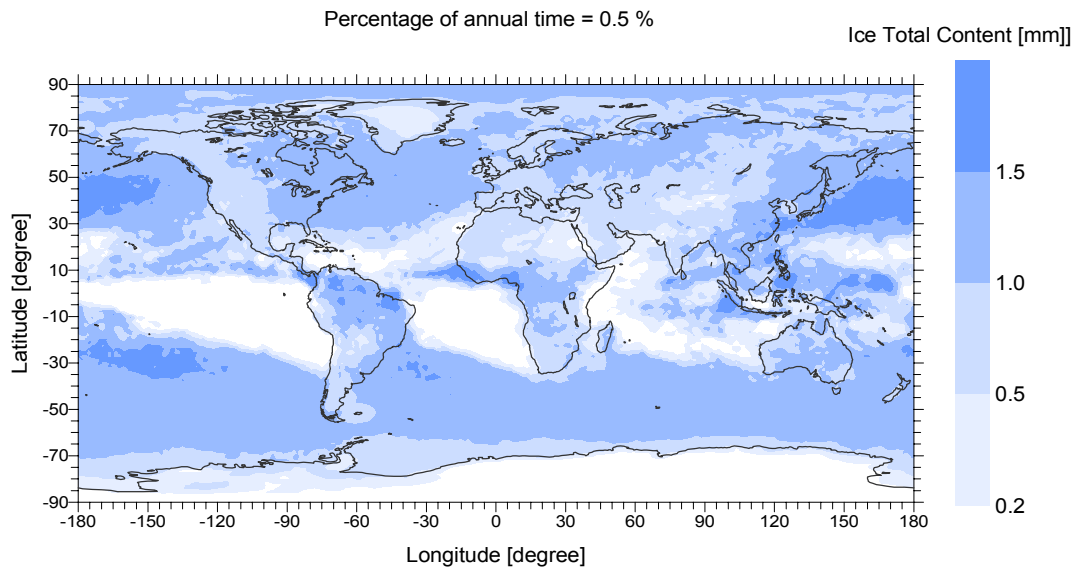


Fig. 1. Global map of the ice total content, [mm], exceeded for the 0.5 % of annual time, derived from ECMWF data

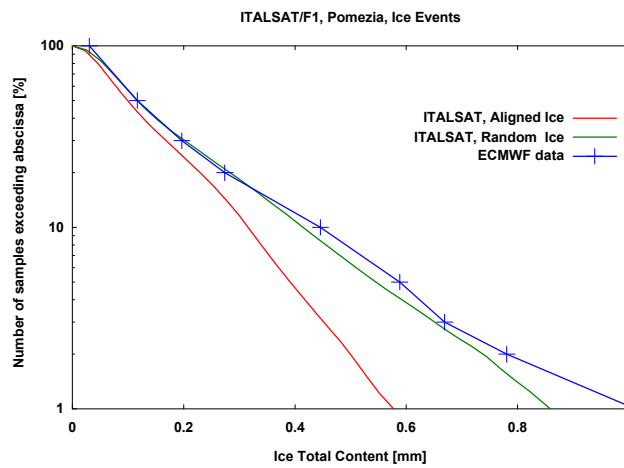


Fig. 2. Comparison between the statistics of Ice total content [mm] in clouds derived from ITALSAT measurements in Pomezia, Italy, and from the ECMWF data (normalised to annual percentage of ice clouds occurrence).

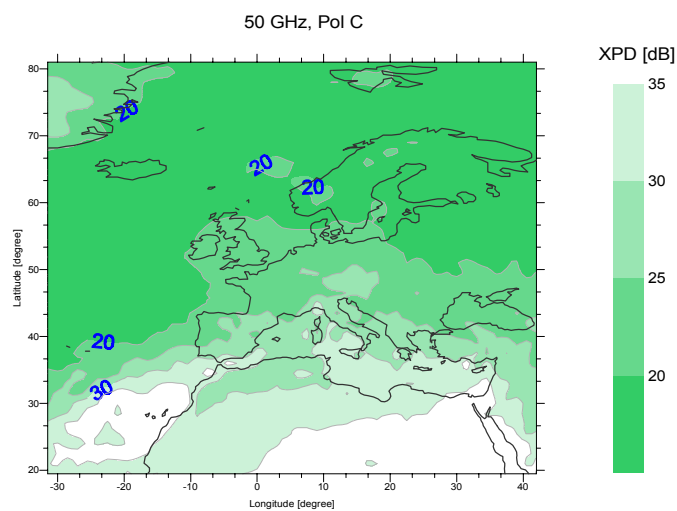


Fig. 3. Map of the crosspolar discrimination, XPD [dB], of circular polarization at 50 GHz exceeded for the 1 % of annual time derived from ECMWF data. The geostationary satellite is located at 13 [deg] E